

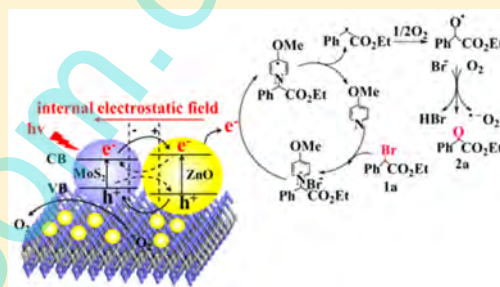
Utilization of MoS₂ Nanosheets To Enhance the Photocatalytic Activity of ZnO for the Aerobic Oxidation of Benzyl Halides under Visible Light

Nan Tian, Zhen Li, Danyun Xu, Yang Li, Wenchao Peng,* Guoliang Zhang, Fengbao Zhang,* and Xiaobin Fan*

School of Chemical Engineering and Technology, State Key Laboratory of Chemical Engineering, Collaborative Innovation Center of Chemical Science and Engineering, Tianjin University, Tianjin 300072, China

S Supporting Information

ABSTRACT: Semiconductors are the low cost and recyclable photocatalysts for visible-light photoredox catalysis, which is one of the prospective ways to convert solar energy to chemical energy in organic synthesis. This study reports a new MoS₂/ZnO composite for the aerobic oxidation of benzyl halides under visible light. Despite the limited intrinsic activity of the ZnO alone, we found that the introduction of a small amount of MoS₂ nanosheets (4 wt %) could significantly improve the catalytic performances of the ZnO in visible-light photoredox catalysis.



INTRODUCTION

Visible-light photoredox catalysis has recently emerged as a powerful tool in synthetic organic chemistry, because the visible light accounts for the major part of the “infinitely available” sunlight.^{1–3} The conversion of solar energy to chemical energy via photocatalysis technology represents a promising solution for addressing both the energy crisis and the climate problem.^{4–6} This approach relies on the ability of the photocatalysts to engage the electron-transfer processes with organic substrates upon photoexcitation with visible light. In previous reports, many homogeneous photocatalysts, especially ruthenium or iridium complexes and organic dyes, have been widely used in many organic catalytic reactions as photocatalysts.^{7–9} However, their high costs and difficulty in reusability and recycling hampered their utilization in practice. Therefore, many efforts have been devoted to semiconductor photocatalysts in recent years.^{10–12} Despite the wide use of the inorganic semiconductors for the photocatalytic degradation of organic waste,^{13–16} the successful examples in which they are used in organic synthesis are still limited, and the photocatalytic performance of these heterogeneous catalysts is still far from satisfactory. To achieve superior photocatalytic activity, the semiconductor should have adequate band-edge positions, large specific surface area, low electron–hole recombination rate, and high carrier mobility.^{17–19} ZnO has been widely used as a promising heterogeneous photocatalyst due to its low cost, nontoxicity, excellent stability, and abundance.^{20–22} However, its visible-light-absorption ability is limited, owing to its relatively wide band gap (about 3.37 eV).^{23–26} Besides, pure ZnO exhibits poor photocatalytic activity because of its quick recombination of photogenerated electron–hole pairs.^{27,28} Doping noble metals as cocatalysts, such as Ag, Pt, and Au,

can increase its photocatalytic activity obviously.^{29–31} However, these metals are rare and expensive to apply on an industrial scale. To explore low cost cocatalysts is a big challenge for developing highly efficient ZnO-based photocatalysts.

Molybdenum disulfide (MoS₂) is an emerging photocatalytic cocatalyst material that may be used as a substitute for noble metals in photocatalyst synthesis.^{32–35} MoS₂ can absorb the visible light effectively due to its narrow band gap (1.3–1.8 eV, depending on the layer numbers). Previous reports have shown that layered MoS₂ with a high exposure edge exhibits much higher activity than noble metals.³⁶

In this study, we prepared MoS₂/ZnO composites via a two-step hydrothermal method and investigated their photocatalytic performances in the aerobic oxidation of benzyl halides driven by visible light. The products are important intermediates for pharmaceuticals and organic synthesis.³⁷ The intimate interface (p–n junction) between ZnO and MoS₂ is proposed to be responsible for the enhanced light absorption from UV (ultraviolet) to visible light. Moreover, due to the excellent electron conductivity and large surface area of MoS₂, the recombination of photoinduced electron–hole pairs can be effectively suppressed. The introduction of a small amount of MoS₂ nanosheets could therefore significantly improve the catalytic performances of the ZnO for aerobic oxidation of benzyl halides.

Received: April 13, 2016

Revised: June 13, 2016

Accepted: July 18, 2016

Published: July 18, 2016

EXPERIMENTAL SECTION

Synthesis of Chemically Exfoliated MoS₂. Single-layer or few-layer MoS₂ was prepared by a chemical exfoliation method.³⁸ One gram of MoS₂ powder was added into 10 mL of *n*-butyllithium solution (1.6 M in hexane) in a 50 mL Schlenk flask. The process was carried out in a glovebox filled with inert gas. Then the mixture was sonicated for 180 min at room temperature. Successively, the dispersion was centrifuged at 13 000 rpm for 15 min to obtain the solid samples, and then the precipitates were washed three times with *n*-hexane to remove the organic residues and excess lithium. Then the samples were dried with argon blowing, followed by sonication in distilled water for about 30 min. The exfoliated samples were washed by centrifugation with deionized water. Finally, the washed solid (the chemically exfoliated MoS₂ nanosheets) was lyophilized for further use.

Synthesis of MoS₂/ZnO composites. MoS₂/ZnO composites were fabricated via the hydrothermal route. NaOH and Zn(CH₃COO)₂ were dissolved in 20 mL of deionized water under magnetic stirring as the molar ratio of 10:1. A 0.01 g sample of as-prepared MoS₂ nanosheets was dissolved in 10 mL of deionized water and sonicated for 30 min, and then it was slowly added into the above solution, followed by stirring for 10 min. The resulting suspension was transferred into a 50 mL Teflon-lined stainless steel autoclave, which was maintained at 160 °C for 6 h. After the reaction, the autoclave was cooled to room temperature naturally. Subsequently, the precipitates were collected by centrifuging and washed several times with deionized water and ethanol. Finally, the obtained precipitates were dried at 80 °C for 8 h in a vacuum. Then we weighed the solid sample to confirm the mass ratio of MoS₂ and ZnO in the nanocomposite. We changed the ratio of MoS₂ and ZnO via controlling the weight of NaOH and Zn(CH₃COO)₂ with the same molar ratio of 10:1, while the weight of the MoS₂ and other experimental conditions were kept the same. The different samples were synthesized with 25, 15, 5, 4, 3, and 2 wt % MoS₂; the corresponding molar ratios of ZnO to MoS₂ were 5.9, 11.2, 37.5, 47.4, 63.9, and 96.8.

Photocatalytic Experiments. The photocatalytic performances of the as-prepared samples were evaluated through the aerobic oxidation of benzyl halides. The reaction was carried out in a Schlenk tube with oxygen as the oxidizing agent and a 24 W compact fluorescent bulb as the light source. As-prepared MoS₂/ZnO composite (10 mg), Li₂CO₃ (74 mg), and 4-methoxyppyridine (22 mg, 0.2 mmol) were added into DMA (dimethylacetamide) (15 mL), and ethyl α -bromo(phenyl)acetate (243 mg, 1 mmol) was added subsequently. In aerobic conditions, the suspensions were exposed to visible light irradiation, and stirring. After 24 h, the catalyst was separated by filtration, and the determination of the reaction product was carried out with GC (gas chromatography) using the external standard method.

Characterization. The samples were characterized by scanning electron microscopy (SEM; Hitachi S4800), transmission electron microscopy (TEM; JEM-2100F), X-ray photoelectron spectroscopy (XPS; PerkinElmer, PHI1600 spectrometer), X-ray diffraction (XRD; AXS D8-Focus), ultraviolet–visible spectrophotometry (Cary 60 UV–vis), atomic force microscopy (AFM; CSPM 5000), Raman spectroscopy (Renishaw in Via reflex Raman spectrometer with 532 nm laser excitation), and steady state fluorescence spectrometry (Jobin Yvon Fluorolog 3-21). The catalytic

reactions were monitored by a GC (Agilent 6890N GC-FID system).

RESULTS AND DISCUSSION

The MoS₂ nanosheets were prepared via the chemical exfoliation method of our previous study.³⁸ Preliminary study confirmed that the 1T phase of the as-prepared MoS₂ nanosheets could be successfully converted to the desired 2H phase under hydrothermal conditions, due to the metastable nature of the 1T phase.³⁹ To prepare the MoS₂/ZnO composites, a mixture of the MoS₂ nanosheets, NaOH, and Zn(CH₃COO)₂ was added into a 50 mL Teflon-lined stainless steel autoclave with 30 mL of deionized water and reacted at 160 °C for 6 h. The ZnO nanoparticles were in situ grown on the surfaces of the MoS₂ nanosheets during the solvothermal process.

X-ray diffraction (XRD) was used to characterize the crystalline structures of the samples. Figure 1 shows the XRD

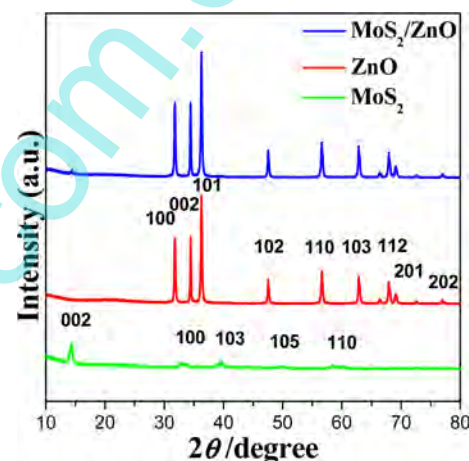


Figure 1. XRD patterns of MoS₂, ZnO, and MoS₂/ZnO composite with MoS₂ loading of 4 wt %.

spectra of MoS₂ nanosheets, ZnO, and the representative MoS₂/ZnO composite with a MoS₂ loading of 4 wt %. Several well-defined diffraction reflections characteristic of ZnO were clearly observed in both the ZnO and MoS₂/ZnO composite samples. The peaks appearing at 31.6, 34.4, 36.1, 47.6, 56.7, 62.9, 68.0, 69.2, and 77.5° can be assigned to the (100), (002), (101), (102), (110), (103), (112), (201), and (202) planes of the hexagonal wurtzite ZnO (JCPDS 36-1451), respectively. Note that a small peak at about 14° can be also observed in the MoS₂/ZnO composite, corresponding to the (002) plane of the restacked MoS₂. Compared with the MoS₂ sample alone, the characteristic (002) peak of the MoS₂ in the composite is significantly lower, attributed to its small content and reduced stacking.

The Raman spectra of the materials are given in Figure 2. Excited with the 532 nm laser, the Raman spectrum of MoS₂ showed two prominent peaks around 376 (E_{2g}¹) and 402 cm⁻¹ (A_{1g}), which was in agreement with the previous report.⁴⁰ Three peaks at 99 cm⁻¹ (E₂), 333 cm⁻¹ (A₁), and 438 cm⁻¹ (E₂) were identified as the characteristic peaks of ZnO.⁴¹ The spectra for MoS₂/ZnO composites contained all the characteristic peaks of MoS₂ and ZnO, indicating the successful combination of them. The chemical composition of the obtained materials can also be characterized by XPS. As shown in Figure 3, all of the peaks for Zn, O, Mo, and S can be

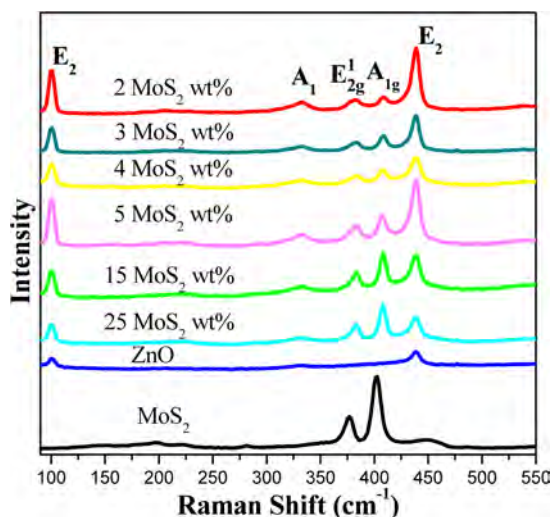


Figure 2. Raman spectra of MoS₂, ZnO, and MoS₂/ZnO composite with different ratios.

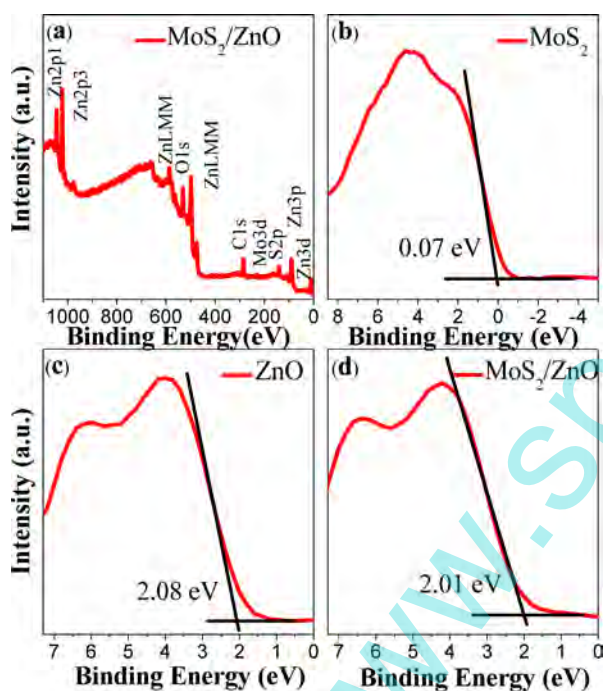


Figure 3. XPS spectrum of (a) MoS₂/ZnO composite. Valence band spectra of (b) chemically exfoliated MoS₂, (c) ZnO, and (d) MoS₂/ZnO composite.

observed in Figure 3a. It can be calculated from the XPS results that the valence band positions of MoS₂, ZnO, and MoS₂/ZnO were 0.07 eV (Figure 3b), 2.08 eV (Figure 3c), and 2.01 eV (Figure 3d), separately. By modification with MoS₂, the valence band of ZnO can be decreased obviously due to the close contact between these two materials.

The morphologies and microstructure of the samples were characterized by scanning electron microscopy (SEM) and transmission electron microscopy (TEM). Figure 4a shows a typical SEM image of the exfoliated MoS₂ nanosheets which show curled edges and smooth surface as reported in previous studies.⁴² On the contrary, the MoS₂/ZnO composite shows a flake-like structure with a rough surface and abundant nanoparticles on its both sides (Figure 4b). This conclusion

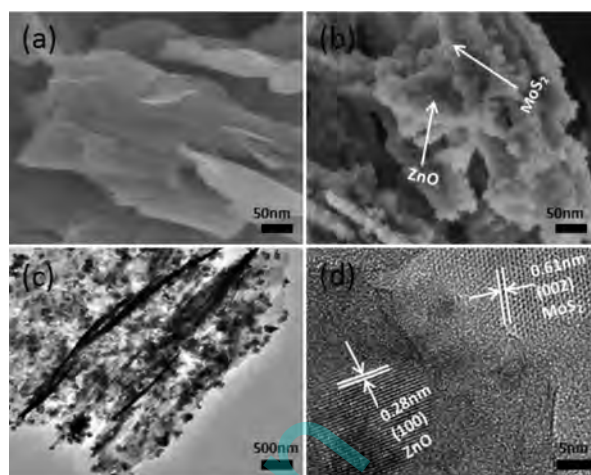


Figure 4. SEM images of (a) MoS₂ nanosheets and (b) MoS₂/ZnO composite. (c) TEM image of MoS₂/ZnO composite. (d) HRTEM of MoS₂/ZnO composite.

is further supported by TEM. As shown in Figure 4c, the ZnO nanoparticles with sizes in the range 20–30 nm were well deposited on the surfaces of the translucent MoS₂ nanosheets. Note that no ZnO nanoparticles outside the MoS₂ nanosheets can be observed, owing to the strong binding and interaction between the ZnO nanoparticles and MoS₂ nanosheets. A close look by HRTEM (high resolution transmission electron microscopy) at their contact region shows the clear lattice spacing of 0.28 and 0.61 nm, corresponding to the (100) plane of ZnO and the (002) plane of hexagonal MoS₂, respectively. All these results confirm the successful preparation of the MoS₂/ZnO composite. The SEM results for other samples with different MoS₂ content are shown in Figure S3 of the Supporting Information. It can be found that the size of ZnO nanoparticles increased gradually with decreasing weight percent MoS₂.

To probe the optical properties of the obtained composites, a variety of the composites with different loadings of the MoS₂ were prepared and systematically characterized by UV–vis diffuse reflectance spectroscopy. As shown in Figure 5, pure ZnO showed photoabsorption properties only in the UV light

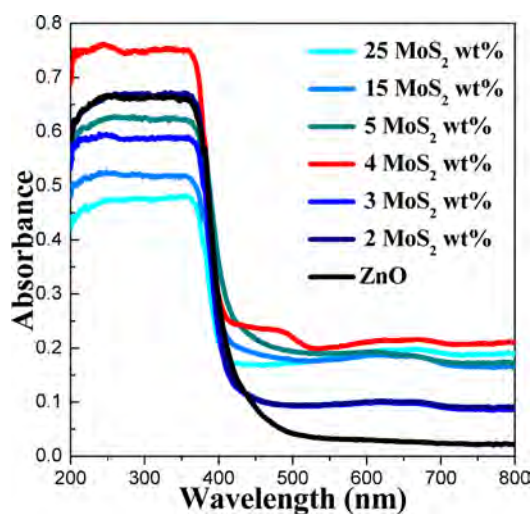


Figure 5. UV–vis absorption spectra of ZnO and MoS₂/ZnO with different mass ratios.

region, which can be explained by its intrinsic band gap energy absorption (3.37 eV). The UV–vis absorption spectrum of MoS₂ is shown in Figure S4 in the Supporting Information, and the band gap of it was calculated to be 1.8 eV according to Figure S5. However, an obvious red shift in the absorption edge was observed after the loading of a small amount of MoS₂. Interestingly, the absorbance of the composite in the visible-light region increases quickly and reaches a plateau when the loading of MoS₂ is 4 wt %, whereas the absorption in the UV region increases first and then decreases. These results can be attributed to the strong absorbance of MoS₂ in the visible-light region. For the sample with limited MoS₂, it is unable to provide enough surface area; consequently, the excessive ZnO cannot form the heterojunction with the MoS₂. By contrast, the redundant ZnO may be agglomerated on the surface, which will decrease the absorbance ability, especially in the visible-light region.

To further study the optical properties of the MoS₂/ZnO composite with the optimized MoS₂ mass ratio of 4 wt %, a comparison study on the PL (photoluminescence) emission was also carried out. It is well-known that PL emission is due to the recombination of excited electrons and holes. The lower PL intensity may indicate the lower recombination rate of electrons and holes under light illumination. On the contrary, the higher PL intensity may manifest the higher recombination rate of electrons and holes, which is the negative factor for the photocatalytic performance.^{43–46} We tested the PL spectra of these composites in the range 450–800 nm.^{47,48} The results are shown in Figure 6. For ZnO, MoS₂, and the MoS₂/ZnO

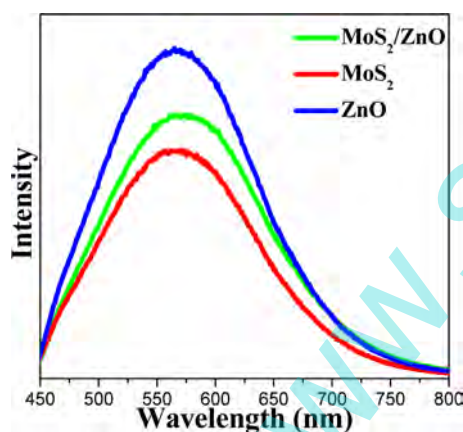


Figure 6. PL spectra of ZnO, MoS₂, and MoS₂/ZnO composite with MoS₂ loading of 4 wt %.

composite samples, they all show a broad visible band from 550 to 600 nm but with obvious changes in intensity. Specifically, ZnO has the highest PL intensity among the three samples, indicating a high recombination of electrons and holes. To our delight, the emission intensity significantly decreases when a suitable amount of MoS₂ was loaded, implying that the recombination of photogenerated carriers was effectively suppressed. The PL spectra of other samples with different MoS₂ contents are shown in the Supporting Information (Figure S1).

The catalytic performance of the obtained MoS₂/ZnO composite was evaluated toward the aerobic oxidation of benzyl halide (Scheme 1), and several control experiments were performed for comparison purposes. As summarized in Table 1, when no catalyst or light was present, limited yields were

Scheme 1. Photocatalyzed Aerobic Oxidation of Ethyl α -Bromo(phenyl)acetate



Table 1. Photocatalyzed Aerobic Oxidation of Ethyl α -Bromo(phenyl)acetate^a

entry	catalyst	MoS ₂ /wt %	yield ^b /%	selectivity/%
1	blank	0	14	25
2	MoS ₂ /ZnO ^c	4	20	23
3	MoS ₂	1	22	28
4	ZnO	0	23	25
5	MoS ₂ /ZnO	25	32	48
6	MoS ₂ /ZnO	15	38	52
7	MoS ₂ /ZnO	5	46	62
8	MoS ₂ /ZnO	4	60	81
9	MoS ₂ /ZnO	3	36	46
10	MoS ₂ /ZnO	2	35	45

^aStandard conditions: α -bromo(phenyl)acetate (1.0 mmol), Li₂CO₃ (1.0 mmol), 4-methoxyppyridine (0.2 mmol), and catalyst (10 mg) were added in DMA (15 mL) under air at 25 °C. Irradiation time using a 24 W compact fluorescent bulb at 20 cm was 24 h. ^bCalibrated yields determined by GC using external standard method. ^cThe reaction was carried out in the dark.

observed for the desired product. Actually, the parallel experiments with ZnO and MoS₂ alone show little improvement. To our surprise, after being combined with MoS₂, the ZnO showed obviously enhanced catalytic activity. In line with the UV–vis absorption results, the MoS₂/ZnO composite with MoS₂ of 4 wt % shows the best performances, and its yield and selectivity for the desired product increased to 60% and 81%, respectively. The reusability of MoS₂/ZnO composite was also evaluated by repeating the same reaction procedure using the recovered catalyst. The solid catalyst was recycled by centrifuging the residue mixture, washing with ethanol repeatedly, and drying in vacuum at 80 °C for 6 h. As shown in Figure 7, the catalyst could be reused for at least five cycles without a distinct loss of its catalytic activity. All these results showed the high photocatalytic activity and good stability of the MoS₂/ZnO composite.

Although the specific mechanisms for the observed enhanced performances remain unclear, it is generally accepted that the photocatalytic process is mainly related to the increased light absorbance and the improved electron–hole pair separation. It has been proven that the MoS₂/ZnO composite with an optimized mass ratio shows excellent optical absorbance from the UV to the visible region. Importantly, the recombination of photogenerated carriers of the ZnO can be also effectively suppressed by the introduction of a small amount of MoS₂. The increasing absorbance of the MoS₂/ZnO composite in the visible-light region should be caused by the MoS₂ ingredient in the composite. Since MoS₂ has a narrow band gap, it can act as a macromolecular organic dye-like photosensitizer in the MoS₂/ZnO composite.¹⁵ Subsequently, ZnO can utilize visible light effectively after sensitization.^{23,24} Due to the intimate

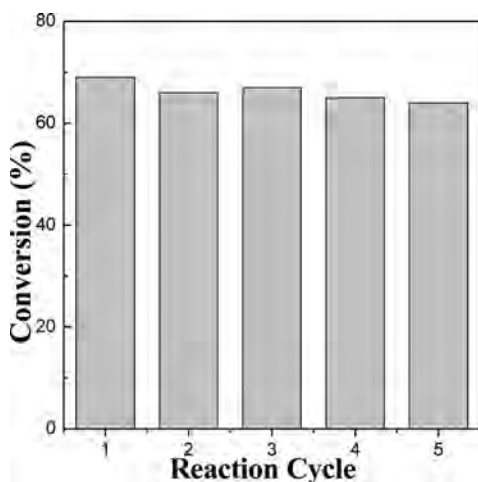
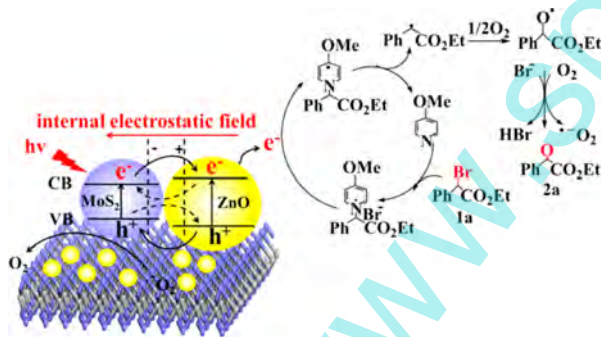


Figure 7. Recyclability of MoS₂/ZnO composite in aerobic photo-oxidation of benzyl halides.

contact in the heterojunction structure, the electrons in the ZnO nanoparticles can diffuse to the MoS₂ at the interface because of the carrier density gradient, forming the positive charge region. Similarly, the holes diffuse to the ZnO from the MoS₂, which consequently forms the negative charge region. According to previous studies, the positive and negative charge regions will generate an internal electrostatic field and band bending, which is significant for the separation of the electron–hole pairs.⁴⁹ As shown in Scheme 2, owing to the presence of

Scheme 2. Proposed Mechanisms for the Enhanced Photocatalytic Activity of the MoS₂/ZnO Composite in the Oxidation of Ethyl α -Bromo(phenyl)acetate



the internal electrostatic field, the photoexcited electrons on the conduction band of the MoS₂ can easily transfer to that of ZnO; undoubtedly, the excited holes on the valence band of ZnO transfer to that of MoS₂. Thus, the photogenerated electrons and holes can be efficiently separated at the interface of the MoS₂/ZnO composite, and enhanced photocatalytic performances in the oxidation of ethyl α -bromo(phenyl)acetate were observed.⁵⁰ In addition, the increased specific surface area because of the two-dimensional feature can promote the photocatalytic abilities to some degree.

CONCLUSIONS

In conclusion, we have developed a new approach to prepare the MoS₂/ZnO composite. By variation of the loading of the MoS₂ nanosheets, the optimized MoS₂/ZnO composite shows much better optical properties and significantly enhanced photocatalytic performances in the visible-light-driven aerobic

oxidation of benzyl halides. We also demonstrated that the composite catalyst could be readily recycled and reused without obvious decline of its photocatalytic activity. This work provides a promising, low-cost, recyclable photocatalyst for visible-light photoredox catalysts.

ASSOCIATED CONTENT

Supporting Information

The Supporting Information is available free of charge on the ACS Publications website at DOI: 10.1021/acs.iecr.6b01420.

PL spectra of all the samples with different MoS₂ contents; AFM image of MoS₂; SEM images of other samples with different MoS₂ contents; UV–vis absorption spectrum of MoS₂; reaction kinetic data; full PL spectrum of MoS₂/ZnO composite (PDF)

AUTHOR INFORMATION

Corresponding Authors

*E-mail: wenchao.peng@tju.edu.cn (W.P.).

*E-mail: fbzhang@tju.edu.cn (F.Z.).

*E-mail: xiaobinfan@tju.edu.cn (X.F.).

Notes

The authors declare no competing financial interest.

ACKNOWLEDGMENTS

This study is supported by the National Natural Science Funds for Excellent Young Scholars (No. 21222608), the Foundation for the Author of National Excellent Doctoral Dissertation of China (No. 201251), the Program for New Century Excellent Talents in University (No. NCET-12-0392), and the Program of Introducing Talents of Discipline to Universities (No. B06006).

REFERENCES

- (1) Schultz, D. M.; Yoon, T. P. Solar synthesis: prospects in visible light photocatalysis. *Science* **2014**, *343*, 1239176.
- (2) Xuan, J.; Xiao, W. J. Visible-light photoredox catalysis. *Angew. Chem., Int. Ed.* **2012**, *51*, 6828.
- (3) Reckenthäler, M.; Griesbeck, A. G. Photoredox Catalysis for Organic Syntheses. *Adv. Synth. Catal.* **2013**, *355*, 2727.
- (4) Lewis, N. S.; Nocera, D. G. Powering the planet: chemical challenges in solar energy utilization. *Proc. Natl. Acad. Sci. U. S. A.* **2006**, *103*, 15729.
- (5) Kudo, A.; Miseki, Y. Heterogeneous photocatalyst materials for water splitting. *Chem. Soc. Rev.* **2009**, *38*, 253.
- (6) Tong, H.; Ouyang, S.; Bi, Y.; Umezawa, N.; Oshikiri, M.; Ye, J. Nano-photocatalytic Materials: Possibilities and Challenges. *Adv. Mater.* **2012**, *24*, 229.
- (7) Zhu, S.; Das, A.; Bui, L.; Zhou, H.; Curran, D. P.; Rueping, M. Oxygen switch in visible-light photoredox catalysis: radical additions and cyclizations and unexpected C–C bond cleavage reactions. *J. Am. Chem. Soc.* **2013**, *135*, 1823.
- (8) Terrett, J. A.; Clift, M. D.; MacMillan, D. W. Direct beta-alkylation of aldehydes via photoredox organocatalysis. *J. Am. Chem. Soc.* **2014**, *136*, 6858.
- (9) Yoon, T. P.; Ischay, M. A.; Du, J. Visible light photocatalysis as a greener approach to photochemical synthesis. *Nat. Chem.* **2010**, *2*, 527.
- (10) Chhowalla, M.; Shin, H. S.; Eda, G.; Li, L. J.; Loh, K. P.; Zhang, H. The chemistry of two-dimensional layered transition metal dichalcogenide nanosheets. *Nat. Chem.* **2013**, *5*, 263.
- (11) Gong, Y.; Lin, J.; Wang, X.; Shi, G.; Lei, S.; Lin, Z.; Zou, X.; Ye, G.; Vajtai, R.; Yakobson, B. I.; Terrones, H.; Terrones, M.; Tay, B. K.; Lou, J.; Pantelides, S. T.; Liu, Z.; Zhou, W.; Ajayan, P. M. Vertical and

in-plane heterostructures from WS₂/MoS₂ monolayers. *Nat. Mater.* **2014**, *13*, 1135.

(12) Vu, T. T. D.; Mighri, F.; Ajji, A.; Do, T.-O. Synthesis of Titanium Dioxide/Cadmium Sulfide Nanosphere Particles for Photocatalyst Applications. *Ind. Eng. Chem. Res.* **2014**, *53*, 3888.

(13) Li, J.; Liu, X.; Pan, L.; Qin, W.; Chen, T.; Sun, Z. MoS₂-reduced graphene oxide composites synthesized via a microwave-assisted method for visible-light photocatalytic degradation of methylene blue. *RSC Adv.* **2014**, *4*, 9647.

(14) Moussa, H.; Giroto, E.; Mozet, K.; Alem, H.; Medjahdi, G.; Schneider, R. ZnO rods/reduced graphene oxide composites prepared via a solvothermal reaction for efficient sunlight-driven photocatalysis. *Appl. Catal., B* **2016**, *185*, 11.

(15) Feng, Y.; Feng, N.; Wei, Y.; Zhang, G. An *in situ* gelatin-assisted hydrothermal synthesis of ZnO-reduced graphene oxide composites with enhanced photocatalytic performance under ultraviolet and visible light. *RSC Adv.* **2014**, *4*, 7933.

(16) Xu, C.; Rangaiah, G. P.; Zhao, X. S. Photocatalytic Degradation of Methylene Blue by Titanium Dioxide: Experimental and Modeling Study. *Ind. Eng. Chem. Res.* **2014**, *53*, 14641.

(17) Macak, J. M.; Zlamal, M.; Krysa, J.; Schmuki, P. Self-organized TiO₂ nanotube layers as highly efficient photocatalysts. *Small* **2007**, *3*, 300.

(18) Xiang, Q.; Yu, J.; Jaroniec, M. Synergetic effect of MoS₂ and graphene as cocatalysts for enhanced photocatalytic H₂ production activity of TiO₂ nanoparticles. *J. Am. Chem. Soc.* **2012**, *134*, 6575.

(19) Akhavan, O. Graphene Nanomesh by ZnO Nanorod Photocatalysts. *ACS Nano* **2010**, *4*, 4174.

(20) Lv, T.; Pan, L.; Liu, X.; Sun, Z. Enhanced photocatalytic degradation of methylene blue by ZnO-reduced graphene oxide-carbon nanotube composites synthesized via microwave-assisted reaction. *Catal. Sci. Technol.* **2012**, *2*, 2297.

(21) Bai, X.; Wang, L.; Zong, R.; Lv, Y.; Sun, Y.; Zhu, Y. Performance Enhancement of ZnO Photocatalyst via Synergic Effect of Surface Oxygen Defect and Graphene Hybridization. *Langmuir* **2013**, *29*, 3097.

(22) Thangavel, S.; Krishnamoorthy, K.; Krishnaswamy, V.; Raju, N.; Kim, S. J.; Venugopal, G. Graphdiyne-ZnO Nanohybrids as an Advanced Photocatalytic Material. *J. Phys. Chem. C* **2015**, *119*, 22057.

(23) Pawar, R. C.; Lee, C. S. Single-step sensitization of reduced graphene oxide sheets and CdS nanoparticles on ZnO nanorods as visible-light photocatalysts. *Appl. Catal., B* **2014**, *144*, 57.

(24) Bu, Y.; Chen, Z.; Li, W.; Hou, B. Highly efficient photocatalytic performance of graphene-ZnO quasi-shell-core composite material. *ACS Appl. Mater. Interfaces* **2013**, *5*, 12361.

(25) Wu, A.; Jing, L.; Wang, J.; Qu, Y.; Xie, Y.; Jiang, B.; Tian, C.; Fu, H. ZnO-dotted porous ZnS cluster microspheres for high efficient, Pt-free photocatalytic hydrogen evolution. *Sci. Rep.* **2015**, *5*, 8858.

(26) Sun, J.; Wan, S.; Wang, F.; Lin, J.; Wang, Y. Selective Synthesis of Methanol and Higher Alcohols over Cs/Cu/ZnO/Al₂O₃ Catalysts. *Ind. Eng. Chem. Res.* **2015**, *54*, 7841.

(27) Xu, T.; Zhang, L.; Cheng, H.; Zhu, Y. Significantly enhanced photocatalytic performance of ZnO via graphene hybridization and the mechanism study. *Appl. Catal., B* **2011**, *101*, 382.

(28) Kumar, S. G.; Rao, K. S. R. K. Zinc oxide based photocatalysis: tailoring surface-bulk structure and related interfacial charge carrier dynamics for better environmental applications. *RSC Adv.* **2015**, *5*, 3306.

(29) Gao, P.; Liu, Z.; Sun, D. D. The synergetic effect of sulfonated graphene and silver as co-catalysts for highly efficient photocatalytic hydrogen production of ZnO nanorods. *J. Mater. Chem. A* **2013**, *1*, 14262.

(30) He, L.; Li, L.; Wang, T.; Gao, H.; Li, G.; Wu, X.; Su, Z.; Wang, C. Fabrication of Au/ZnO nanoparticles derived from ZIF-8 with visible light photocatalytic hydrogen production and degradation dye activities. *Dalton Trans.* **2014**, *43*, 16981.

(31) Peng, T.-y.; Lv, H.-j.; Zeng, P.; Zhang, X.-h. Preparation of ZnO Nanoparticles and Photocatalytic H₂ Production Activity from

Different Sacrificial Reagent Solutions. *Chin. J. Chem. Phys.* **2011**, *24*, 464.

(32) Najmaei, S.; Liu, Z.; Zhou, W.; Zou, X.; Shi, G.; Lei, S.; Yakobson, B. I.; Idrobo, J. C.; Ajayan, P. M.; Lou, J. Vapour phase growth and grain boundary structure of molybdenum disulphide atomic layers. *Nat. Mater.* **2013**, *12*, 754.

(33) Maitra, U.; Gupta, U.; De, M.; Datta, R.; Govindaraj, A.; Rao, C. N. Highly effective visible-light-induced H₂ generation by single-layer 1T-MoS₂ and a nanocomposite of few-layer 2H-MoS₂ with heavily nitrogenated graphene. *Angew. Chem., Int. Ed.* **2013**, *52*, 13057.

(34) Lopez-Sanchez, O.; Lembke, D.; Kayci, M.; Radenovic, A.; Kis, A. Ultrasensitive photodetectors based on monolayer MoS₂. *Nat. Nanotechnol.* **2013**, *8*, 497.

(35) Chang, K.; Mei, Z.; Wang, T.; Kang, Q.; Ouyang, S.; Ye, J. MoS₂/Graphene Cocatalyst for Efficient Photocatalytic H₂ Evolution under Visible Light Irradiation. *ACS Nano* **2014**, *8*, 7078.

(36) Hou, Y.; Laursen, A. B.; Zhang, J.; Zhang, G.; Zhu, Y.; Wang, X.; Dahl, S.; Chorkendorff, I. Layered nanojunctions for hydrogen-evolution catalysis. *Angew. Chem., Int. Ed.* **2013**, *52*, 3621.

(37) Xie, Y.; Liu, J.; Huang, Y.; Yao, L. A novel method for synthesis of α -keto esters with phenyliodine(III) diacetate. *Tetrahedron Lett.* **2015**, *56*, 3793.

(38) Fan, X.; Xu, P.; Zhou, D.; Sun, Y.; Li, Y. C.; Nguyen, M. A.; Terrones, M.; Mallouk, T. E. Fast and Efficient Preparation of Exfoliated 2H MoS₂ Nanosheets by Sonication-Assisted Lithium Intercalation and Infrared Laser-Induced 1T to 2H Phase Reversion. *Nano Lett.* **2015**, *15*, 5956.

(39) Chou, S. S.; Huang, Y. K.; Kim, J.; Kaehr, B.; Foley, B. M.; Lu, P.; Dykstra, C.; Hopkins, P. E.; Brinker, C. J.; Huang, J.; Dravid, V. P. Controlling the metal to semiconductor transition of MoS₂ and WS₂ in solution. *J. Am. Chem. Soc.* **2015**, *137*, 1742.

(40) Xu, J.; Cao, X. Characterization and mechanism of MoS₂/CdS composite photocatalyst used for hydrogen production from water splitting under visible light. *Chem. Eng. J.* **2015**, *260*, 642.

(41) Cuscó, R.; Alarcón-Lladó, E.; Ibáñez, J.; Artús, L.; Jiménez, J.; Wang, B.; Callahan, M. J. Temperature dependence of Raman scattering in ZnO. *Phys. Rev. B: Condens. Matter Mater. Phys.* **2007**, *75*, 165202.

(42) Chen, Y. T.; Tian, G.; Shi, Y.; Xiao, Y.; Fu, H. Hierarchical MoS₂/Bi₂MoO₆ composites with synergistic effect for enhanced visible photocatalytic activity. *Appl. Catal., B* **2015**, *164*, 40.

(43) Wang, F.; Liang, L.; Shi, L.; Liu, M.; Sun, J. CO₂-assisted synthesis of mesoporous carbon/C-doped ZnO composites for enhanced photocatalytic performance under visible light. *Dalton Trans.* **2014**, *43*, 16441.

(44) Liu, C.; Wang, L.; Tang, Y.; Luo, S.; Liu, Y.; Zhang, S.; Zeng, Y.; Xu, Y. Vertical single or few-layer MoS₂ nanosheets rooting into TiO₂ nanofibers for highly efficient photocatalytic hydrogen evolution. *Appl. Catal., B* **2015**, *164*, 1.

(45) Liqiang, J.; Yichun, Q.; Baiqi, W.; Shudan, L.; Baojiang, J.; Libin, Y.; Wei, F.; Honggang, F.; Jiazhong, S. Review of photoluminescence performance of nano-sized semiconductor materials and its relationships with photocatalytic activity. *Sol. Energy Mater. Sol. Cells* **2006**, *90*, 1773.

(46) Hu, C.; Zheng, S.; Lian, C.; Chen, F.; Lu, T.; Hu, Q.; Duo, S.; Zhang, R.; Guan, C. α -S nanoparticles grown on MoS₂ nanosheets: A novel sulfur-based photocatalyst with enhanced photocatalytic performance. *J. Mol. Catal. A: Chem.* **2015**, *396*, 128.

(47) Zhang, K.; Zhang, Y.; Zhang, T.; Dong, W.; Wei, T.; Sun, Y.; Chen, X.; Shen, G.; Dai, N. Vertically coupled ZnO nanorods on MoS₂ monolayers with enhanced Raman and photoluminescence emission. *Nano Res.* **2015**, *8*, 743.

(48) Wang, Y.; Sun, M.; Fang, Y.; Sun, S.; He, J. Ag₂S and MoS₂ as dual, co-catalysts for enhanced photocatalytic degradation of organic pollutions over CdS. *J. Mater. Sci.* **2016**, *51*, 779.

(49) Tan, Y.-H.; Yu, K.; Li, J.-Z.; Fu, H.; Zhu, Z.-Q. MoS₂@ZnO nano-heterojunctions with enhanced photocatalysis and field emission properties. *J. Appl. Phys.* **2014**, *116*, 064305.

(50) Su, Y.; Zhang, L.; Jiao, N. Utilization of Natural Sunlight and Air in the Aerobic Oxidation of Benzyl Halides. *Org. Lett.* **2011**, *13*, 2168.

www.spm.com.cn